the centre of the perfect crystal (*A–B–A* stacking) is replaced by an inversion centre at the midpoint of the single rhombohedral cell *A–B–C*; the projected symmetry is also reduced from hexagonal to trigonal: both whole pattern and central beam then have the symmetry of $3m1$. The $2H$ polytype of TaS_2 ($P6_3/mmc$) (Tanaka & Terauchi, 1985) gives a second clear example. (*b*) In the case of a [111] gold crystal, sectioning the f.c.c. structure parallel to [111] preparatory to producing the twin already reduces the finite crystal symmetry to $R\bar{3}m$, *i.e.* a trigonal space group for which the central beam, and the HOLZ reflections in particular, exhibit the trigonal symmetry of $31m$ (rather than the $3m1$ of trigonal graphite). A central-plane twin boundary with no associated translation introduces a central horizontal mirror plane into the crystal. For the zone-axis pattern the only symmetry change will be in the central beam, which will become centrosymmetric, increasing its symmetry to $6mm$. Using diffraction-group terminology these cases are seen to be relative inverses. Unfaulted graphite has the BESR group $6mm1_R$ (central beam and whole pattern hexagonal); central-plane faulting results in a change to the group 6_Rmm_R. Unfaulted [111] gold correspondingly has the BESR group symmetry 6_Rmm_R; central-plane twinning results in the addition of the element 1_R (for a central mirror plane), leading to the group $6mm1_R$.

(iv) Finally, no present-day discussion of electron-crystallographic investigations of symmetry could be complete without reference to two aspects of non-classical symmetries widely discussed in the literature in recent years. The recent discovery of noncrystallographic point symmetries in certain alloys (Shechtman *et al.*, 1984) has led to the study of quasi-crystallinity. An excellent record of the experimental side of this subject may be found in the book *Convergent-beam electron diffraction III* by Tanaka *et al.* (1994), while the appropriate space-group theory has been developed by Mermin (1992). It would be inappropriate to comment further on this new subject here other than to state that this is clearly an area of study where combined HREM, CBED and selected-area diffraction (SAD) evidence is vital to structural elucidation.

The other relatively new topic is that of modulated structures. From experimental evidence, two distinct structural phenomena can be distinguished for structures exhibiting incommensurate superlattice reflections. Firstly, there are 'Vernier' phases, which exist within certain composition ranges of solid solutions and are composed of two extensive substructures, for which the superspace-group nomenclature developed by de Wolff *et al.* (1981) is structurally valid (*e.g.* Withers *et al.*, 1993). Secondly, there are structures essentially composed of random mixtures of two or more substructures existing as microdomains within the whole crystal (*e.g.* Grzinic, 1985). Here the SAD patterns will contain superlattice reflections with characteristic profiles and/or irregularities of spacings. A well illustrated review of incommensurate-structure analysis in general is given in the book by Tanaka *et al.* (1994), while specific discussions of this topic are given by Goodman *et al.* (1992), and Goodman & Miller (1993).

2.5.3.7. *Present limitations and general conclusions*

The list of examples given here must necessarily be regarded as unsatisfactory considering the vastness of the subject, although some attempt has been made to choose a diverse range of problems which will illustrate the principles involved. Some particular aspects, however, need further mention.

One of these concerns the problem of examining large-unit-cell materials with a high diffraction-pattern density. This limits the possible convergence angle, if overlap is to be avoided, and leaves numerous but featureless discs [for example Goodman (1984*b*)]. Technical advances which have been made to overcome this problem include the beam-rocking technique (Eades, 1980) and LACBED (Tanaka *et al.*, 1980), both of which are reviewed by Tanaka & Terauchi (1985) and Eades *et al.* (1983). The disadvantage of these latter methods is that they both require a significantly larger area of specimen than does the conventional technique, and it may be that more sophisticated methods of handling the crowded conventional patterns are still needed.

Next, the matter of accuracy must be considered. There are two aspects of the subject where this is of concern. Firstly, there is a very definite limit to the sensitivity with which symmetry can be detected. In a simple structure of medium-light atoms, displacements of say 0.1 Å or less from a pseudomirror plane could easily be overlooked. An important aspect of CBED analysis, not mentioned above, is the *N*-beam computation of patterns which is required when something approaching a refinement (in the context of electron diffraction) is being attempted. Although this quantitative aspect has a long history [for example see Johnson (1972)], it has only recently been incorporated into symmetry studies as a routine (Creek & Spargo, 1985; Tanaka, 1994). Multi-slice programs which have been developed to produce computer-simulated pattern output are available (Section 2.5.3.8).

Next there is concern as to the allocation of a space group to structures which microscopically have a much lower symmetry (Goodman *et al.*, 1984). This arises because the volume sampled by the electron probe necessarily contains a large number of unit cells. Reliable microscopic interpretation of certain nonstoichiometric materials requires that investigations be accompanied by high-resolution microscopy. Frequently (especially in mineralogical samples), nonstoichiometry implies that a space group exists only on average, and that the concept of absolute symmetry elements is inapplicable.

From earlier and concluding remarks it will be clear that combined X-ray/CBED and CBED/electron-microscopy studies of inorganic materials represents the standard ideal approach to space-group analysis at present; given this approach, all the space-group problems of classical crystallography appear soluble. As has been noted earlier, it is important that HREM be considered jointly with CBED in determining space group by electron crystallography, and that only by this joint study can the so-called 'phase problem' be completely overcome. The example of the space-group pairs $I222/I2_12_12_1$ and $I23/I2_13$ has already been cited. Using CBED, it might be expected that FOLZ lines would show a break from twofold symmetry with the incident beam aligned with a 2_1 axis. However, a direct distinction should be made apparent from high-resolution electron micrographs. Other less clear-cut cases occur where the HREM images allow a space-group distinction to be made between possible space groups of the same arithmetic class, especially when only one morphology is readily obtained (*e.g.* $P222_1$, $P22_12_1$, $P2_12_12_1$).

The slightly more subtle problem of distinguishing enantiomorphic space-group pairs can be solved by one of two approaches: either the crystal must be rotated around an axis by a known amount to obtain two projections, or the required three-dimensional phase information can be deduced from specific three-beam-interaction data. This problem is part of the more general problem of solving handedness in an asymmetric structure, and is discussed in detail by Johnson & Preston (1994).

2.5.3.8. *Computer programs available*

(1) A FORTRAN source listing of program *TCBED* for simulating three-dimensional convergent-beam patterns with absorption by the Bloch-wave method: Zuo *et al.* (1989) [see also *Electron microdiffraction* (Spence & Zuo, 1992) for other useful programs and worked examples for the analysis of these diffraction

(*continued on page* 306)

Table 2.5.3.4. *Tabulation of principal-axis CBED pattern symmetries against relevant space groups given as IT A numbers*

Three columns of diperiodic groups (central section) correspond to (i) symmorphic groups, (ii) non-symmorphic groups (GS bands) and (iii) non-symmorphic groups (zero-layer absences arising from horizontal glide planes). Cubic space groups are given underlined in the right-hand section with the code: underlining = [001](cyclic) setting; italics + underlining = [110](cyclic) setting. Separators ';' and ':' indicate change of Bravais lattice type and change of crystal system, respectively.

	I Point groups		II Diperiodic groups				III Space groups
DG	H–M	BESR	(i)	(ii)	(iii)	SG	Subgroups II*b* (Subgroups 1)
Oblique						Triclinic	
1	1	1	$p1$			1	
2*	$\bar{1}$	2_R	$p\bar{1}'$			2	
						Monoclinic (Oblique)	
3	12	2	$p2$			3	4, 5
4	$1m$	1_R	pm'			6	8
5	$1m$				pb'	7	9
6*	$2/m$	21_R	$p2/m'$			10	11, 12
7*	$2/m$	21_R			$p2/b'$	13	14, 15
Rectangular						(Rectangular)	
8	21	m_R	$p2'$			3	5^2: *195*; *197*, *199*
9	21	m_R		$p2_1'$		4	*198*
10	21	m_R	$c2'$			5	*196*
11	$m1$	m	pm			6^2	7, 8^2
12	$m1$	m		pa		7^2	9^2
13	$m1$	m	cm			8	9
14*	$12/m$	2_Rmm_R	$p2'/m$			10	13, 12^2: *200*, *201*; *204*
15*	$12/m$	2_Rmm_R		$p2_1'/m$		11	14
16*	$12/m$	2_Rmm_R		$p2'/a$		13^2	15^2: *206*
17*	$12/m$	2_Rmm_R		$p2_1'/m$		14^2	*205*
18*	$12/m$	2_Rmm_R	$c2'/m$			12	15: *202*, *203*
						Orthorhombic	
19	222	$2m_Rm_R$	$p2'2'2$			16	17; 21^2; 22: 195; 196, *207*, *206*; *211*, *214*
20	222	$2m_Rm_R$		$p2_1'2'2$		17^2	18^2; 20^2: *212*, *213*
21	222	$2m_Rm_R$		$p2_1'2_1'2$		18	19: 198
22	222	$2m_Rm_R$	$c2'2'2$			21	20; 23, 24: 197, 199, *209*, *210*
23	$mm2$	$2mm$	$pmm2$			25	26, 27; 38, 39; 42
24	$mm2$	$2mm$		$pbm2$		28	29, 30, 31^2; 40, 41
25	$mm2$	$2mm$		$pba2$		32	33, 34; 43
26	$mm2$	$2mm$	$cmm2$			35	36, 37; 44, 45, 46
27	$mm2$	$m1_R$	$p2'mm'$			25^2	28^1; 35^2, 42^2; 38^2, 39^2: *215*; *217*
28	$mm2$	$m1_R$		$p2_1'm'a$		26^1	31^1; 36^1
29	$mm2$	$m1_R$		$p2_1'ab'$	$(p2_1'ab')$	29^2	33^2
30	$mm2$	$m1_R$			$p2_1'ma'$	26^2	29^1; 36^2
31	$mm2$	$m1_R$			$p2_1'mn'$	31^2	33^2
32	$mm2$	$m1_R$			$p2'mb'$	28^2	32^2, 40^2, 41^2
33	$mm2$	$m1_R$			$p2'aa'$	27^2	30^2; 37^2
34	$mm2$	$m1_R$			$pb2'n'$	30^1	34^2; 43^2: *218*; *219*
35	$mm2$	$m1_R$	$c2'mm'$			38^1	40^1; 44^2, 46^1: *216*; *220*
36	$mm2$	$m1_R$			$c2'mb'$	39^1	41^1; 45^2, 46^2
37*	mmm	$2mm1_R$	$pmmm'$			47	49, 51^1; 65^2, 67^2; 69: *200*; *202*, *221*, *224*, *226*, *228*, *229*
38*	mmm	$2mm1_R$		$pbmm'$ $(2_1')$		51^2	53^1, 57, 59^2; 63^1, 64^1
39*	mmm	$2mm1_R$		$pbam'$ $(2_1'2_1')$		55	58, 62^2
40*	mmm	$2mm1_R$		$pmab'$ $(2_1'2_1')$	$(pmab')$	57^1	60^2, 61, 62: 205
41*	mmm	$2mm1_R$		$pbaa'$ $(2_1')$	$(pbaa')$	54^2	52, 56^2, 60^1

Table 2.5.3.4. *Tabulation of principal-axis CBED pattern symmetries against relevant space groups given as IT A numbers* (*cont.*)

	I Point groups		II Diperiodic groups				III Space groups
DG	H–M	BESR	(i)	(ii)	(iii)	SG	Subgroups II*b* (Subgroups 1)
42*	*mmm*	$2mm1_R$			$pmma'$ $(2'_1)$	51	54, 55^2, 57^2; 63^2, 64^2
43*	*mmm*	$2mm1_R$			$pmmn'$ $(2'_12'_1)$	59	56, 62^1
44*	*mmm*	$2mm1_R$			$pbmn'$ $(2'_1)$	53^2	52^1, 58^1, 60
45*	*mmm*	$2mm1_R$			$pmaa'$	49^2	50^2, 53, 54^1; 66^2, 68^1: 222, 223
46*	*mmm*	$2mm1_R$			$pban'$	50	52^2, 48; 70: 201; 203, 230
47*	*mmm*	$2mm1_R$	$cmmm'$			65	63, 66; 72, 74^2, 71: 204, 225, 227
48*	*mmm*	$2mm1_R$			$cmma'$	67	64, 68; 72^1, 74, 73: 206
Square						Tetragonal	
49	4	4	$p4$			75	77, 76, 78; 79, 80
50	$4/m$	41_R	$p4/m'$			83	84; 87
51	$4/m$	41_R			$p4/n'$	85	86, 88
52	422	$4m_Rm_R$	$p42'2'$			89	93, 91, 95; 97, 98: 207, 208; 209, 210; 211, 214
53	422	$4m_Rm_R$		$p42'_12'$		90	94, 92, 96: 212, 213
54	$4mm$	$4mm$	$p4mm$			99	101, 103, 105; 107, 108
55	$4mm$	$4mm$		$p4bm$		100	102, 104, 106; 109, 110
56*	$4/mmm$	$4mm1_R$	$p4/m'mm$			123	124, 131, 132; 139, 140; 221, 223; 225, 226; 229
57*	$4/mmm$	$4mm1_R$		$p4/m'bm$ $(2'_1)$		127	128, 135, 136
58*	$4/mmm$	$4mm1_R$			$p4/n'bm$	125	126, 133, 134; 141, 142: 222, 224; 227, 228; 230
59*	$4/mmm$	$4mm1_R$			$p4/n'mm$ $(2'_1)$	129	130, 137, 138
60	$\bar{4}$	4_R	$p\bar{4}'$			81	82
61	$\bar{4}2m$	4_Rmm_R	$p\bar{4}'m\bar{2}'$			115	116; 119, 120
62	$\bar{4}2m$	4_Rmm_R		$p\bar{4}b2'$		117	118; 122: 220
63	$\bar{4}2m$	4_Rmm_R	$p\bar{4}'2'm$			111	112; 121: 215; 216; 217; 218; 219
64	$\bar{4}2m$	4_Rmm_R		$p4'2'_1m$		113	114
Hexagonal						Trigonal	
65	3	3	$p3$			143	144, 145; 146
66	$\bar{3}$	6_R	$p\bar{3}'$			147	148
67	32	$3m_R$	$p312'$			149	151, 153
68	32	$3m_R$	$p32'1$			150	152, 154; 155
69	$3m$	$3m$	$p31m$			157	159
70	$3m$	$3m$	$p3m1$			156	158; 160, 161
71*	$\bar{3}m$	6_Rmm_R	$p\bar{3}'1m$			162	163
72*	$\bar{3}m$	6_Rmm_R	$p\bar{3}'m1$			164	165; 166, 167
						Hexagonal	
73	6	6	$p6$			168	171, 172, 173, 169, 170
74	$\bar{6}$	31_R	$p3/m'$ $(p\bar{6}')$			174	
75	622	$6m_Rm_R$	$p62'2'$			177	180, 181, 182, 178, 179
76	$6mm$	$6mm$	$p6mm$			183	184, 185, 186
77*	$6/m$	61_R	$p6/m'$			175	176
78*	$6/mmm$	$6mm1_R$	$p6/m'mm$			191	192, 193, 194
79	$\bar{6}m2$	$3m1_R$	$p3/m'2'm$ $(p\bar{6}'m2')$			189	190
80	$\bar{6}m2$	$3m1_R$	$p3/m'm2'$ $(p\bar{6}'2'm)$			187	188

Table 2.5.3.5. *Conditions for observation of GS bands for the 137 space groups exhibiting these extinctions*

Point groups 2, *m*, 2/*m* (2nd setting unique axis $\|b$)

Space group		Incident-beam direction [$u0w$]
4	$P2_1$	$0k0$ 2_1 S
7	Pc	$h0l$ c G
9	Cc	$h0l$ c G
11	$P2_1/m$	$0k0$ 2_1 S
13	$P2/c$	$h0l$ c G
14	$P2_1/c$	$0k0$ 2_1 S $h0l$ c G
15	$C2/c$	$h0l$ c G

Point groups 222, *mm*2

Space group		Incident-beam direction					
		[100]	[010]	[001]	[$uv0$]	[$0vw$]	[$u0w$]
17	$P222_1$	$00l$ 2_1 S	$00l$ 2_1 S		$00l$ 2_1 S		
18	$P2_12_12$	$0k0$ 2_1 S	$h00$ 2_1 S	$h00$, $0k0$ 2_1 S		$h00$ 2_1 S	$0k0$ 2_1 S
19	$P2_12_12_1$	$0k0$, $00l$ 2_1 S	$h00$, $00l$ 2_1 S	$h00$, $0k0$ 2_1 S	$00l$ 2_1 S	$h00$ 2_1 S	$0k0$ 2_1 S
20	$C222_1$	$00l$ 2_1 S	$00l$ 2_1 S		$00l$ 2_1 S		
26	$Pmc2_1$	$00l$ $c+2_1$ GS	$00l$ 2_1 $c'-$		$00l$ 2_1 S		$h0l$ c G
27	$Pcc2$	$00l$ c $c'-$	$00l$ c $c'-$			$0kl$ c G	$h0l$ c G
28	$Pma2$			$h00$ a G			$h0l$ a G
29	$Pca2_1$	$00l$ 2_1 $c'-$	$00l$ $c+2_1$ GS	$h00$ a G	$00l$ 2_1 S	$0kl$ c G	$h0l$ a G
30	$Pnc2$	$00l$ c $n'-$	$00l$ n $c'-$	$0k0$ n G		$0kl$ n G	$h0l$ c G
31	$Pmn2_1$	$00l$ $n+2_1$ GS	$00l$ 2_1 $n'-$	$h00$ n G	$00l$ 2_1 S		$h0l$ n G
32	$Pba2$			$h00$, $0k0$ a b G		$0kl$ b G	$h0l$ a G

Table 2.5.3.5. *Conditions for observation of GS bands for the 137 space groups exhibiting these extinctions* (*cont.*)

Space group		Incident-beam direction					
		[100]	[010]	[001]	[uv0]	[0vw]	[u0w]
33	$Pna2_1$	00l 2_1 $n'-$	00l $n+2_1$ GS	h00, 0k0 a b G	00l 2_1 S	0kl n G	h0l a G
34	$Pnn2$	00l n $n'-$	00l n $n'-$	h00, 0k0 n G		0kl n G	h0l n G
36	$Cmc2_1$	00l $c+2_1$ GS	00l 2_1 $c'-$		00l 2_1 S		h0l c G
37	$Ccc2$	00l c $c'-$	00l c $c'-$			0kl c G	h0l c G
39	$Abm2$					0kl b G	
40	$Ama2$			h00 a G			h0l a G
41	$Aba2$			h00 a G		0kl b G	h0l a G
43	$Fdd2$	00l $d'-$	00l d $d'-$	h00, 0k0 d G		0kl d G	h0l d G
45	$Iba2$	$b'-$	$a'-$			0kl b G	h0l a G
46	$Ima2$		$a'-$				h0l a G

Point group *mmm*

Space group		Incident-beam direction					
		[100]	[010]	[001]	[uv0]	[0vw]	[u0w]
48	$P\,2/n\,2/n\,2/n$	00l, 0k0 n $n'-$	00l, h00 n $n'-$	0k0, h00 n $n'-$	hk0 n G	0kl n G	h0l n G
49	$P\,2/c\,2/c\,2/m$	00l c $c'-$	00l c $c'-$			0kl c G	h0l c G
50	$P\,2/b\,2/a\,2/n$	0k0 n $b'-$	h00 n $a'-$	0k0, h00 b a $n'-$	hk0 n G	0kl b G	h0l a G
51	$P\,2_1/m\,2/m\,2/a$		h00 $a+2_1$ GS	h00 2_1 $a'-$	hk0 a G	h00 2_1 S	
52	$P\,2/n\,2_1/n\,2/a$	00l, 0k0 n 2_1 $a'-$	00l, h00 n a $n'-$	0k0 $n+2_1$ GS h00 n $n'-$	hk0 a G	0kl n G	h0l n G 0k0 2_1 S
53	$P\,2/m\,2/n\,2_1/a$	00l $n+2_1$ GS	h00, 00l a 2_1 $a'-$	h00 n $a'-$	hk0 a G 00l 2_1 S		h0l n G

Table 2.5.3.5. *Conditions for observation of GS bands for the 137 space groups exhibiting these extinctions* (*cont.*)

Space group		Incident-beam direction					
		[100]	[010]	[001]	[*uv*0]	[0*vw*]	[*u*0*w*]
54	$P\,2_1/c\,2/c\,2/a$	$00l$ c $c'-$	$h00$ $a+2_1$ *GS* $00l$ c $c'-$	$h00$ 2_1 $a'-$	$hk0$ a *G*	$0kl$ c *G* $h00$ 2_1 *S*	$h0l$ c *G*
55	$P\,2_1/b\,2_1/a\,2/m$	$0k0$ 2_1 $b'-$	$h00$ 2_1 $a'-$	$0k0, h00$ $b+2_1, a+2_1$ *GS*		$0kl$ b *G* $h00$ 2_1 *S*	$h0l$ a *G* $0k0$ 2_1 *S*
56	$P\,2_1/c\,2_1/c\,2/n$	$0k0$ $n+2_1$ *GS* $00l$ c $c'-$	$h00$ $n+2_1$ *GS* $00l$ c $c'-$	$0k0, h00$ 2_1 $n'-$	$hk0$ n *G*	$0kl$ c *G* $h00$ 2_1 *S*	$h0l$ c *G* $0k0$ 2_1 *S*
57	$P\,2/b\,2_1/c\,2_1/m$	$00l$ $c+2_1$ *GS* $0k0$ 2_1 $b'-$	$00l$ 2_1 $c'-$	$0k0$ $b+2_1$ *GS*	$00l$ 2_1 *S*	$0kl$ b *G*	$h0l$ c *G* $0k0$ 2_1 *S*
58	$P\,2_1/n\,2_1/n\,2/m$	$00l, 0k0$ $n\quad 2_1$ $n'-$	$00l, h00$ $n\quad 2_1$ $n'-$	$0k0, h00$ $n+2_1$ *GS*		$0kl$ n *G* $h00$ 2_1 *S*	$h0l$ n *G* $0k0$ 2_1 *S*
59	$P\,2_1/m\,2_1/m\,2/n$	$0k0$ $n+2_1$ *GS*	$h00$ $n+2_1$ *GS*	$0k0, h00$ 2_1 $n'-$	$hk0$ n *G*	$h00$ 2_1 *S*	$0k0$ 2_1 *S*
60	$P\,2_1/b\,2/c\,2_1/n$	$00l$ $c+2_1$ *GS* $0k0$ n $b'-$	$h00$ $n+2_1$ *GS* $00l$ 2_1 $c'-$	$0k0, h00$ $b\quad 2_1$ $n'-$	$hk0$ n *G* $00l$ 2_1 *S*	$0kl$ b *G* $h00$ 2_1 *S*	$h0l$ c *G*
61	$P\,2_1/b\,2_1/c\,2_1/a$	$00l$ $c+2_1$ *GS* $0k0$ 2_1 $b'-$	$h00$ $a+2_1$ *GS* $00l$ 2_1 $c'-$	$0k0$ $b+2_1$ *GS* $h00$ 2_1 $a'-$	$hk0$ a *G* $00l$ 2_1 *S*	$0kl$ b *G* $h00$ 2_1 *S*	$h0l$ c *G* $0k0$ 2_1 *S*
62	$P\,2_1/n\,2_1/m\,2_1/a$	$0k0, 00l$ 2_1 $n'-$	$00l$ $n+2_1$ *GS* $h00$ $a+2_1$	$0k0$ $n+2_1$ *GS* $h00$ 2_1 $a'-$	$hk0$ a *G* $00l$ 2_1 *S*	$0kl$ n *G* $h00$ 2_1 *S*	$0k0$ 2_1 *S*
63	$C\,2/m\,2/c\,2_1/m$	$00l$ $c+2_1$ *GS*	$00l$ 2_1 $c'-$		$00l$ 2_1 *S*		$h0l$ c *G*
64	$C\,2/m\,2/c\,2_1/a$	$00l$ $c+2_1$ *GS*	$00l$ 2_1 $c'-$		$hk0$ a *G* $00l$ 2_1 *S*		$h0l$ c *G*
66	$C\,2/c\,2/c\,2/m$	$00l$ c $c'-$	$00l$ c $c'-$			$0kl$ c *G*	$h0l$ c *G*
67	$C\,2/m\,2/m\,2/a$				$hk0$ a *G*		

Table 2.5.3.5. *Conditions for observation of GS bands for the 137 space groups exhibiting these extinctions* (*cont.*)

Space group		Incident-beam direction											
		[100]		[010]		[001]		[*uv*0]		[0*vw*]		[*u*0*w*]	
68	*C* 2/*c* 2/*c* 2/*a*	00*l* *c*	*c*′–	00*l* *c*	*c*′–			*hk*0 *a*	*G*	0*kl* *c*	*G*	*h*0*l* *c*	*G*
70	*F* 2/*d* 2/*d* 2/*d*	00*l*, 0*k*0 *d*	*d*′–	*h*00, 00*l* *d*	*d*′–	0*k*0, *h*00 *d*	*d*′–	*hk*0 *d*	*G*	0*kl* *d*	*G*	*h*0*l* *d*	*G*
72	*I* 2/*b* 2/*a* 2/*m*		*b*′–		*a*′–					0*kl* *b*	*G*	*h*0*l* *a*	*G*
73	*I* 2/*b* 2/*c* 2/*a*		*b*′–		*c*′–		*a*′–	*hk*0 *a*	*G*	0*kl* *b*	*G*	*h*0*l* *c*	*G*
74	*I* 2/*m* 2/*m* 2/*a*							*hk*0 *a*	*G*				

Point groups 4, $\bar{4}$, 4/*m*

Space group		Incident-beam direction	
		[*uv0*]	
76	$P4_1$	00*l* 4_1	*S*
78	$P4_3$	00*l* 4_3	*S*
85	$P4/n$	*hk*0 *n*	*G*
86	$P4_2/n$	*hk*0 *n*	*G*
88	$I4_1/a$	*hk*0 *a*	*G*

Point group 422

Space group		Incident-beam direction			
		[*uv0*]		[0*vw*]	
90	$P42_12$			*h*00 2_1	*S*
91	$P4_122$	00*l* 4_1	*S*		
92	$P4_12_12$	00*l* 4_1	*S*	*h*00 2_1	*S*
94	$P4_22_12$			*h*00 2_1	*S*
95	$P4_322$	00*l* 4_3	*S*		
96	$P4_32_12$	00*l* 4_3	*S*	*h*00 2_1	*S*

Point group 4*mm*

Space group		Incident-beam direction									
		[100]		[001]		[110]		[*u*0*w*] and [0*vw*]*		[*uūw*]	
100	*P*4*bm*			*h*00, 0*k*0 *a* *b*	*G*			*h*0*l*, 0*kl* *a* *b*	*G*		
101	$P4_2cm$	00*l* *c*	*c*′–					*h*0*l*, 0*kl* *c*	*G*		
102	$P4_2nm$	00*l* *n*	*n*′–	*h*00, 0*k*0 *n*	*G*			*h*0*l*, 0*kl* *n*	*G*		
103	*P*4*cc*	00*l* *c*	*c*′–			00*l* *c*	*c*′–	*h*0*l*, 0*kl* *c*	*G*	*hhl* *c*	*G*
104	*P*4*nc*	00*l* *n*	*n*′–	*h*00, 0*k*0 *n*	*G*	00*l* *c*	*c*′–	*h*0*l*, 0*kl* *n*	*G*	*hhl* *c*	*G*
105	$P4_2mc$					00*l* *c*	*c*′–			*hhl* *c*	*G*

Table 2.5.3.5. *Conditions for observation of GS bands for the 137 space groups exhibiting these extinctions* (*cont.*)

Space group	Incident-beam direction				
	[100]	[001]	[110]	[*u*0*w*] and [0*vw*]*	[*uūw*]
106 $P4_2bc$		*h*00, 0*k*0 *a* *b* *G*	00*l* *c* *c*′−	*h*0*l*, 0*kl* *a* *b* *G*	*hhl* *c* *G*
108 $I4cm$				*h*0*l*, 0*kl* *c* *G*	
109 $I3_1md$		*hh*0 $\bar{h}h$0 *G* *d*	00*l* *d* *d*′−		*hhl* *G* *d*
110 $I4_1cd$		*hh*0 $\bar{h}h$0 *G* *d*	00*l* *d* *d*′−	*h*0*l*, 0*kl* *G* *c*	*hhl* *G* *d*

* Conditions in this column are cyclic on *h* and *k*.

Point groups $\bar{4}2m$, 4/*mmm*

Space group	Incident-beam direction					
	[100]	[001]	[110]	[*u*0*w*] and [0*vw*]*	[*uuw*]	[*uv*0]
112 $P\bar{4}2c$			00*l* *c* *c*′−		*hhl* *c* *G*	
113 $P\bar{4}2_1m$	0*k*0 2_1 *S*	*h*00, 0*k*0 2_1 *S*		0*k*0, *h*00 2_1 *S*		
114 $P\bar{4}2_1c$	0*k*0 2_1 *S*	*h*00, 0*k*0 2_1 *S*	00*l* *c* *c*′−	0*k*0, *h*00 2_1 *S*	*hhl* *c* *G*	
116 $P\bar{4}c2$	00*l* *c* *c*′−			*h*0*l*, 0*kl* *c* *G*		
117 $P\bar{4}b2$		*h*00, 0*k*0 *a* *b* *G*		*h*0*l*, 0*kl* *a* *b* *G*		
118 $P\bar{4}n2$	00*l* *n* *n*′−	*h*00, 0*k*0 *n* *G*		*h*0*l*, 0*kl* *n* *G*		
120 $I\bar{4}c2$				*h*0*l*, 0*kl* *c* *G*		
122 $I\bar{4}2d$		*hh*0 $\bar{h}h$0 *G* *d*	00*l* *d* *d*′−		*hhl* *G* *d*	
124 $P\,4/m\,2/c\,2/c$	00*l* *c* *c*′−		00*l* *c* *c*′−	*h*0*l*, 0*kl* *c* *G*	*hhl* *c* *G*	
125 $P\,4/n\,2/b\,2/m$	0*k*0 *n* *b*′−	*h*00, 0*k*0 *a* *b* *n*′−		*h*0*l*, 0*kl* *a* *b* *G*		*hk*0 *n* *G*
126 $P\,4/n\,2/n\,2/c$	0*k*0 *n* 00*l* *n* *n*′−	*h*00, 0*k*0 *n* *n*′−	00*l* *c* *c*′−	*h*0*l*, 0*kl* *n* *G*	*hhl* *c* *G*	*hk*0 *n* *G*
127 $P\,4/m\,2_1/b\,2/m$	0*k*0 2_1 *b*′−	*h*00 $a+2_1$ *GS* 0*k*0 $b+2_1$		*h*0*l*, 0*kl* *a* *b* *G* 0*k*0, *h*00 2_1 *S*		

Table 2.5.3.5. *Conditions for observation of GS bands for the 137 space groups exhibiting these extinctions* (*cont.*)

Space group		Incident-beam direction					
		[100]	[001]	[110]	[$u0w$] and [$0vw$]*	[uuw]	[$uv0$]
128	$P\,4/m\,2_1/n\,2/c$	$00l$, $0k0$ n 2_1 $n'-$	$h00$, $0k0$ $n+2_1$ *GS*	$00l$ c $c'-$	$h0l$, $0kl$ n *G* $0k0$, $h00$ 2_1 *S*	hhl c *G*	
129	$P\,4/n\,2_1/m\,2/m$	$0k0$ $n+2_1$ *GS*	$h00$, $0k0$ 2_1 $n'-$		$0k0$, $h00$ 2_1 *S*		$hk0$ n *G*
130	$P\,4/n\,2_1/c\,2/c$	$0k0$ $n+2_1$ *GS* $00l$ c $c'-$	$h00$, $0k0$ 2_1 $n'-$	$00l$ c $c'-$	$h0l$, $0kl$ c *G* $0k0$, $h00$ 2_1 *S*	hhl c *G*	$hk0$ n *G*
131	$P\,4_2/m\,2/m\,2/c$			$00l$ c $c-$		hhl c *G*	
132	$P\,4_2/m\,2/c\,2/m$	$00l$ c $c'-$			$h0l$, $0kl$ c *G*		
133	$P\,4_2/n\,2/b\,2/c$	$0k0$ n $b'-$	$h00$, $0k0$ a b $n'-$	$00l$ c $c'-$	$h0l$, $0kl$ a b *G*	hhl c *G*	$hk0$ n *G*
134	$P\,4_2/n\,2/n\,2/m$	$0k0$, $00l$ n $n'-$	$h00$, $0k0$ n $n'-$		$h0l$, $0kl$ n *G*		$hk0$ n *G*
135	$P\,4_2/m\,2_1/b\,2/c$	$0k0$ 2_1 $b'-$	$h00$, $0k0$ $a+2_1$ $b+2_1$ *GS*	$00l$ c $c'-$	$h0l$, $0kl$ a b *G* $0k0$, $h00$ 2_1 *S*	hhl c *G*	
136	$P\,4_2/m\,2_1/n\,2/m$	$00l$, $0k0$ n 2 $n'-$	$h00$, $0k0$ $n+2_1$ *GS*		$h0l$, $0kl$ n *G* $0k0$, $h00$ 2_1 *S*		
137	$P\,4_2/n\,2_1/m\,2/c$	$0k0$ $n+2_1$ *GS*	$h00$, $0k0$ 2_1 $n'-$	$00l$ c $c'-$	$0k0$, $h00$ 2_1 *S*	hhl c *G*	$hk0$ n *G*
138	$P\,4_2/n\,2_1/c\,2/m$	$0k0$ $n+2_1$ *GS* $00l$ c $c'-$	$h00$, $0k0$ 2_1 $n'-$		$h0l$, $0kl$ c *G* $0k0$, $h00$ 2_1 *S*		$hk0$ n *G*
140	$I\,4/m\,2/c\,2/m$				$h0l$, $0kl$ c *G*		
141	$I\,4_1/a\,2/m\,2/d$		$hh0$ $\bar{h}h0$ d $a'-$	$00l$, $\bar{h}h0$ d a $d'-$		hhl d *G*	$hk0$ a *G*
142	$I\,4_1/a\,2/c\,2/d$		$hh0$ $\bar{h}h0$ d $a'-$	$00l$, $\bar{h}h0$ d a $d'-$	$h0l$, $0kl$ c *G*	hhl d *G*	$hk0$ a *G*

* Conditions in this column are cyclic on h and k.

Table 2.5.3.5. *Conditions for observation of GS bands for the 137 space groups exhibiting these extinctions* (*cont.*)

Point groups 3*m*, $\bar{3}m$, 6, 6/*m*, 622, 6*mm*, $\bar{6}m2$, 6/*mmm*

Space group		Incident-beam direction			
		[100]	[210]	[2*u u w*]	[*v*0*w*]
158	$P3c1$		$000l$ c G	$hh2\bar{h}l$ c G	
159	$P31c$	$000l$ c G			$h\bar{h}0l$ c G
161	$R3c$		$000l$ $l = 6n + 3$ G c	$hh2\bar{h}l$ G c	
163	$P\bar{3}1c$	$000l$ c G			$h\bar{h}0l$ c G
165	$P\bar{3}c1$		$000l$ c G	$hh2\bar{h}l$ c G	
167	$R\bar{3}c$		$000l$ $l = 6n + 3$ G c	$hh2\bar{h}l$ G c	
169	$P6_1$	$000l$ 6_1 S	$000l$ 6_1 S		
170	$P6_5$	$00l$ 6_5 S	$00l$ 6_5 S		
173	$P6_3$	$000l$ 6_3 S	$000l$ 6_3 S		
176	$P6_3/m$	$000l$ 6_3 S	$000l$ 6_3 S		
178	$P6_122$	$000l$ 6_1 S	$000l$ 6_1 S		
179	$P6_522$	$000l$ 6_5 S	$000l$ 6_5 S		
182	$P6_322$	$000l$ 6_3 S	$000l$ 6_3 S		
184	$P6cc$	$000l$ c $c'-$	$000l$ c $c'-$	$hh2\bar{h}l$ c G	$h\bar{h}0l$ c G
185	$P6_3cm$	$000l$ 6_3 $c'-$	$000l$ $c + 6_3$ GS	$hh2\bar{h}l$ c G	
186	$P6_3mc$	$000l$ $c + 6_3$ GS	$000l$ 6_3 $c'-$		$h\bar{h}0l$ c G
188	$P\bar{6}c2$		$000l$ c G	$hh2\bar{h}l$ c G	
190	$P\bar{6}c2$	$000l$ c G			$h\bar{h}0l$ c G
192	$P6/mcc$	$000l$ c $c'-$	$000l$ c $c'-$	$hh2\bar{h}l$ c G	$h\bar{h}0l$ c G
193	$P6_3/mcm$	$00l$ 6_3 $c'-$	$000l$ $c + 6_3$ GS	$hh2\bar{h}l$ c G	
194	$P6_3/mmc$	$000l$ $c + 6_3$ GS	$000l$ 6_3 $c'-$		$h\bar{h}0l$ c G

Table 2.5.3.5. *Conditions for observation of GS bands for the 137 space groups exhibiting these extinctions* (*cont.*)

Point groups 23, *m*3, 432, *m*3*m*

Space group		Incident-beam direction			
		[100] (cyclic)	[110] (cyclic)	[*uv*0] (cyclic)	[*uuw*] (cyclic)
198	$P2_13$	$00l$, $0k0$ 2_1 S	$00l$ 2_1 S	$00l$ 2_1 S	
201	$Pn\bar{3}$ $P2/n\bar{3}$	$00l$, $0k0$ n $n'-$		$\bar{k}h0$ n G	
203	$Pd\bar{3}$ $F2/d\bar{3}$	$00l$, $0k0$ d $d'-$		$\bar{k}h0$ d G	
205	$Pa\bar{3}$ $P2_1/a\bar{3}$	$00l$ $c+2_1$ GS $0k0$ 2_1 $b'-$	$00l$ 2_1 S $\bar{h}h0$ a G	$00l$ 2_1 S $\bar{k}h0$ a G	
206	$Ia\bar{3}$ $I2_1/a\bar{3}$		$\bar{h}h0$ a G	$\bar{k}h0$ a G	
212	$P4_332$			$00l$ 4_3 S	
213	$P4_132$			$00l$ 4_1 S	
218	$P\bar{4}3n$		$00l$ c $n-$	hhl c G	
219	$F\bar{4}3c$			hhl c G	
220	$I\bar{4}3d$	$0kk$ $0\bar{k}k$ d G	$00l$ d $d-$	hhl d G	
222	$Pn\bar{3}n$	$00l$, $0k0$ n $n'-$	$00l$ c $n-$	$hk0$ n G	hhl c G
223	$Pm\bar{3}n$		$00l$ c $n'-$		hhl c G
224	$Pn\bar{3}m$	$00l$, $0k0$ n $n'-$		$hk0$ n G	
226	$Fm\bar{3}c$				hhl c G
227	$Fd\bar{3}m$	$00l$, $0k0$ d $d'-$		$hk0$ d G	
228	$Fd\bar{3}c$	$00l$, $0k0$ d $d'-$		$hk0$ d G	hhl c G
230	$Ia\bar{3}d$	$0kk$ $0\bar{k}k$ d $b'-$	$00l$, $\bar{h}h0$ $d\quad a$ $d'-$	$hk0$ a G	hhl d G

patterns]. Contact J. M. Zuo or J. C. H. Spence, Physics Department, Arizona State University, Tempe, Arizona, USA.

(2) A package for CBED pattern simulation by both Bloch-wave and multi-slice methods is available from P. Stadelmann (pierre.stadelmann@cime.uhd.edfl.ch), Lausanne, Switzerland, in UNIX for workstations [Silicon Graphics, Dec Alpha (OSF), IBM RISC 6000, SUN and HP-9000].

(3) HOLZ line simulations: Listing for PC 8801 (NEC): Tanaka & Terauchi (1985, pp. 174–175).

2.5.4. Electron-diffraction structure analysis (EDSA)

(B. K. VAINSHTEIN AND B. B. ZVYAGIN)

2.5.4.1. *Introduction*

Electron-diffraction structure analysis (EDSA) (Vainshtein, 1964) based on electron diffraction (Pinsker, 1953) is used for the investigation of the atomic structure of matter together with X-ray and neutron diffraction analysis. The peculiarities of EDSA, as compared with X-ray structure analysis, are defined by a strong interaction of electrons with the substance and by a short wavelength λ. According to the Schrödinger equation (see Section 5.2.2) the electrons are scattered by the electrostatic field of an object. The values of the atomic scattering amplitudes, f_e, are three orders higher than those of X-rays, f_x, and neutrons, f_n. Therefore, a very small quantity of a substance is sufficient to obtain a diffraction pattern. EDSA is used for the investigation of very thin single-crystal films, of ~5–50 nm polycrystalline and textured films, and of deposits of finely grained materials and surface layers of bulk specimens. The structures of many ionic crystals, crystal hydrates and hydro-oxides, various inorganic, organic, semiconducting and metallo-organic compounds, of various minerals, especially layer silicates, and of biological structures have been investigated by means of EDSA; it has also been used in the study of polymers, amorphous solids and liquids.

Special areas of EDSA application are: determination of unit cells; establishing orientational and other geometrical relationships between related crystalline phases; phase analysis on the basis of d_{hkl} and I_{hkl} sets; analysis of the distribution of crystallite dimensions in a specimen and inner strains in crystallites as determined from line profiles; investigation of the surface structure of single crystals; structure analysis of crystals, including atomic position determination; precise determination of lattice potential distribution and chemical bonds between atoms; and investigation of crystals of biological origin in combination with electron microscopy (Vainshtein, 1964; Pinsker, 1953; Zvyagin, 1967; Pinsker *et al.*, 1981; Dorset, 1976; Zvyagin *et al.*, 1979).

There are different kinds of electron diffraction (ED) depending on the experimental conditions: high-energy (HEED) (above 30–200 kV), low-energy (LEED) (10–600 V), transmission (THEED), and reflection (RHEED). In electron-diffraction studies use is made of special apparatus – electron-diffraction cameras in which the lens system located between the electron source and the specimen forms the primary electron beam, and the diffracted beams reach the detector without aberration distortions. In this case, high-resolution electron diffraction (HRED) is obtained. ED patterns may also be observed in electron microscopes by a selected-area method (SAD). Other types of electron diffraction are: MBD (microbeam), HDD (high-dispersion), CBD (convergent-beam), SMBD (scanning-beam) and RMBD (rocking-beam) diffraction (see Sections 2.5.2 and 2.5.3). The recent development of electron diffractometry, based on direct intensity registration and measurement by scanning the diffraction pattern against a fixed detector (scintillator followed by photomultiplier), presents a new improved level of EDSA which provides higher precision and reliability of structural data (Avilov *et al.*, 1999; Tsipursky & Drits, 1977; Zhukhlistov *et al.*, 1997, 1998; Zvyagin *et al.*, 1996).

Electron-diffraction studies of the structure of molecules in vapours and gases is a large special field of research (Vilkov *et al.*, 1978). See also *Stereochemical Applications of Gas-Phase Electron Diffraction* (1988).

2.5.4.2. *The geometry of ED patterns*

In HEED, the electron wavelength λ is about 0.05 Å or less. The Ewald sphere with radius λ^{-1} has a very small curvature and is approximated by a plane. The ED patterns are, therefore, considered as plane cross sections of the reciprocal lattice (RL) passing normal to the incident beam through the point 000, to scale $L\lambda$ (Fig. 2.5.4.1). The basic formula is

$$r = |\mathbf{h}|L\lambda, \text{ or } rd = L\lambda, \qquad (2.5.4.1)$$

where r is the distance from the pattern centre to the reflection, $\mathbf{h}$ is the reciprocal-space vector, d is the appropriate interplanar distance and L is the specimen-to-screen distance. The deviation of the Ewald sphere from a plane at distance h from the origin of the coordinates is $\delta_h = h^2\lambda/2$. Owing to the small values of λ and to the rapid decrease of f_e depending on $(\sin\theta)/\lambda$, the diffracted beams are concentrated in a small angular interval (≤ 0.1 rad).

Single-crystal ED patterns image one plane of the RL. They can be obtained from thin ideal crystalline plates, mosaic single-crystal films, or, in the RHEED case, from the faces of bulk single crystals. Point ED patterns can be obtained more easily owing to the following factors: the small size of the crystals (increase in the dimension of RL nodes) and mosaicity – the small spread of crystallite orientations in a specimen (tangential tension of the RL nodes). The crystal system, the parameters of the unit cell and the Laue symmetry are determined from point ED patterns; the probable space group is found from extinctions. Point ED patterns may be used for intensity measurements if the kinematic approximation holds true or if the contributions of the dynamic and secondary scattering are not too large.

The indexing of reflections and the unit-cell determination are carried out according to the formulae relating the RL to the DL (direct lattice) (Vainshtein, 1964; Pinsker, 1953; Zvyagin, 1967).

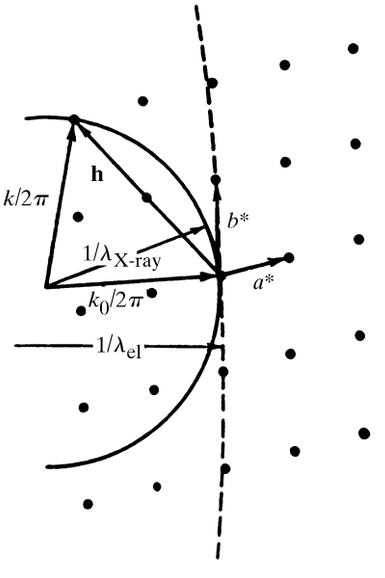

Fig. 2.5.4.1. Ewald spheres in reciprocal space. Dotted line: electrons, solid line: X-rays.

references